

$Y(4626)$ in a chiral constituent quark model

Yue Tan* and Jialun Ping†

*Department of Physics and Jiangsu Key Laboratory for Numerical Simulation of Large Scale Complex Systems,
Nanjing Normal University, Nanjing 210023, P. R. China*

Recently, Belle Collaboration reported a new exotic state $Y(4620)$ with mass at 4625.9 MeV in the positronium annihilation process. Inspired by experiment, we study the tetraquark system $c\bar{s}s\bar{c}$ with quantum numbers $J^P = 1^-$ in the framework of chiral constituent quark model with the help of Gaussian expansion method. Two structures, diquark-antidiquark and meson-meson, with all possible color and spin configurations are considered. The result shows that no bound state can be formed. To investigate the possible resonance states, the real scaling method is employed. Several resonance states with energies 4354, 4408, 4469, 4497 and 4531 MeV, are proposed. Taking into account the errors in calculating the $q\bar{q}$ mesons, the system errors in the calculation of four-quark system are around 60~100 MeV. The resonance with energy 4531 MeV is possible the candidate of the newly found state $Y(4620)$.

PACS numbers:

I. INTRODUCTION

Since the state $X(3872)$ first observed by the Belle collaboration [1], a lot of new hadrons have been reported subsequently the other collaborations [2–8]. Most of them cannot be fitted well in the conventional picture of meson and baryon, which are called exotic states. In fact, the exotic states can be divided into two kinds: the first kind is the states with exotic quantum numbers, and the second one is the states with normal quantum numbers but their properties cannot be described by the conventional quark models. In the picture of quark model, the meson is made up of quark-antiquark and baryon is made up of three quarks. With the accumulation of experimental data on exotic states, people believe that these exotic states can provide much essential information on low energy QCD and help us to establish the effective method to describe all hadrons.

Very recently, the Belle Collaboration observed a new structure, named $Y(4626)$, in the $D_s D_{s1}(2536)$ invariant mass spectrum with 5.9σ significance [9]. The mass and width measured is $M = 4265.9_{-6.0}^{+6.2} \pm 0.4$ MeV and $\Gamma = 49.8_{-11.5}^{+13.9} \pm 4.0$ MeV, respectively. Its decay mode $D_s D_{s1}(2536)$ indicates that $Y(4626)$ is consist of charm and strange quarks. The Belle Collaboration also suggested that the quantum numbers of the state is $J^P = 1^-$. Because the mass is close to the threshold of $D_s + D_{s1}(2536)$, the possible assignment is $c\bar{s}s\bar{c}$ four-quark state.

There were lots of researches about $c\bar{s}s\bar{c}$ before [10–16]. For example, Chen *et al.* analyzed the tetraquark states $c\bar{s}s\bar{c}$ with $J^P = 1^+$ (in S -wave) and $J^P = 0^+$ (in D -wave) within within the framework of QCD sum rules [10]. Deng *et al.* used color flux-tube model to investigate systematically the hidden charmed states observed in re-

cent years including $J^P = 0^+$ and $J^P = 1^+$ $c\bar{s}s\bar{c}$ system [11]. Recently, in the framework of the chiral quark model Yang *et al.* investigated the four-quark system $c\bar{s}s\bar{c}$ with quantum numbers 1^+ and 0^+ , and described the $X(4274)$ and $X(4350)$ states in diquark-antidiquark picture [12]. So far, most of the previous work considered only the four-quark states with negative parity, the four-quark states with $J^P = 1^-$ is nevertheless untouched.

In this paper, a constituent quark model is employed to systematically investigate the $c\bar{s}s\bar{c}$ states with $J^P = 1^-$ with the help of gaussian expansion method. In the calculation, all of possible color and spin configurations are considered. In addition, two structures, meson-meson and diquark-antidiquark and their mixing, are also taken into account. In fact, one structure is complete for the calculation, if all excitation of the structure are taken into account. Clearly it is too difficult to use this approach. An economic way is to combine different structures, which are kept in the low-lying state to do the calculation. In this approach, the problem of over-complete will shown up. To solve the problem, the eigenfunction method is employed. First the overlap matrix is diagonalized, the eigenvectors with eigenvalue 0 are abandoned, then re-constructed the hamiltonian matrix using the remained eigenvectors of overlap matrix. At last, the new hamiltonian matrix is diagonalized to obtained the eigen-energies of the system. In order to keep the matrix manageable, the important structures, meson-meson and diquark-antidiquark structures which are favorable physically, are considered. Other structures, e.g., K-type structure are not favorable, so they are not taken into account temporarily.

The paper is organized as follows. In Sect. II, the chiral quark model and the wave functions of the $c\bar{s}s\bar{c}$ with quantum numbers $J^P = 1^-$ are presented. The numerical results are given in Sec. III. The last section is devoted to the summary of the present work.

*Electronic address: 181001003@stu.njnu.edu.cn

†Electronic address: jlping@njnu.edu.cn(Corresponding author)

II. CHIRAL QUARK MODEL AND WAVE FUNCTION OF $c\bar{s}s\bar{c}$ SYSTEM

A. Chiral quark model

The chiral quark model has been applied successfully in describing the hadron spectra and hadron-hadron interactions. The details of the model can be found in Ref. [17–22]. Here only the Hamiltonian of the chiral quark model for four-quark system is shown,

$$H = \sum_{i=1}^4 m_i + \frac{p_{12}^2}{2\mu_{12}} + \frac{p_{34}^2}{2\mu_{34}} + \frac{p_{1234}^2}{2\mu_{1234}} + \sum_{i<j=1}^4 \left(V_{ij}^C + V_{ij}^G + \sum_{\chi=\pi,K,\eta,\sigma} V_{ij}^\chi \right), \quad (1)$$

where m_i is the constituent mass of i -th quark (antiquark), and μ is the reduced mass of two interacting quarks or quark-clusters.

$$\begin{aligned} \mu_{ij} &= \frac{m_i m_j}{m_i + m_j}, \quad ij = 12, 34 \\ \mu_{1234} &= \frac{(m_1 + m_2)(m_3 + m_4)}{m_1 + m_2 + m_3 + m_4}, \\ p_{ij} &= \frac{m_j p_i - m_i p_j}{m_i + m_j}, \\ p_{1234} &= \frac{(m_3 + m_4)p_{12} - (m_1 + m_2)p_{34}}{m_1 + m_2 + m_3 + m_4}. \end{aligned} \quad (2)$$

V^C is the confining potential, mimics the ‘‘confinement’’ property of QCD,

$$V_{ij}^C = (-a_c r_{ij}^2 - \Delta) \boldsymbol{\lambda}_i^c \cdot \boldsymbol{\lambda}_j^c \quad (3)$$

The second potential V^G is one-gluon exchange interaction reflecting the ‘‘asymptotic freedom’’ property of QCD.

$$\begin{aligned} V_{ij}^G &= \frac{\alpha_s}{4} \boldsymbol{\lambda}_i^c \cdot \boldsymbol{\lambda}_j^c \left[\frac{1}{r_{ij}} - \frac{2\pi}{3m_i m_j} \boldsymbol{\sigma}_i \cdot \boldsymbol{\sigma}_j \delta(\mathbf{r}_{ij}) \right] \\ \delta(\mathbf{r}_{ij}) &= \frac{e^{-r_{ij}/r_0(\mu_{ij})}}{4\pi r_{ij} r_0^2(\mu_{ij})}, \end{aligned} \quad (4)$$

$\boldsymbol{\sigma}$ are the $SU(2)$ Pauli matrices; $\boldsymbol{\lambda}_c$ are $SU(3)$ color Gell-Mann matrices, $r_0(\mu_{ij}) = \frac{r_0}{\mu_{ij}}$ and α_s is an effective scale-dependent running coupling,

$$\alpha_s(\mu_{ij}) = \frac{\alpha_0}{\ln[(\mu_{ij}^2 + \mu_0^2)/\Lambda_0^2]}. \quad (5)$$

The third potential V_χ is Goldstone boson exchange, coming from ‘‘chiral symmetry spontaneous breaking’’ of

TABLE I: Quark model parameters ($m_\pi = 0.7$ fm, $m_\sigma = 3.42$ fm, $m_\eta = 2.77$ fm, $m_K = 2.51$ fm).

Quark masses	$m_u = m_d(\text{MeV})$	313
	$m_s(\text{MeV})$	536
	$m_c(\text{MeV})$	1728
	$m_b(\text{MeV})$	5112
Goldstone bosons	$\Lambda_\pi = \Lambda_\sigma(\text{fm}^{-1})$	4.2
	$\Lambda_\eta = \Lambda_K(\text{fm}^{-1})$	5.2
	$g_{ch}^2/(4\pi)$	0.54
	$\theta_p(^{\circ})$	-15
Confinement	$a_c(\text{MeV})$	101
	$\Delta(\text{MeV})$	-78.3
	$\mu_c(\text{MeV})$	0.7
OGE	α_0	3.67
	$\Lambda_0(\text{fm}^{-1})$	0.033
	$\mu_0(\text{MeV})$	36.976
	$\hat{r}_0(\text{MeV})$	28.17

QCD in the low-energy region,

$$\begin{aligned} V_{ij}^\pi &= \frac{g_{ch}^2}{4\pi} \frac{m_\pi^2}{12m_i m_j} \frac{\Lambda_\pi^2}{\Lambda_\pi^2 - m_\pi^2} m_\pi v_{ij}^\pi \sum_{a=1}^3 \lambda_i^a \lambda_j^a, \\ V_{ij}^K &= \frac{g_{ch}^2}{4\pi} \frac{m_K^2}{12m_i m_j} \frac{\Lambda_K^2}{\Lambda_K^2 - m_K^2} m_K v_{ij}^K \sum_{a=4}^7 \lambda_i^a \lambda_j^a, \\ V_{ij}^\eta &= \frac{g_{ch}^2}{4\pi} \frac{m_\eta^2}{12m_i m_j} \frac{\Lambda_\eta^2}{\Lambda_\eta^2 - m_\eta^2} m_\eta v_{ij}^\eta \\ &\quad [\lambda_i^8 \lambda_j^8 \cos \theta_P - \lambda_i^0 \lambda_j^0 \sin \theta_P], \\ V_{ij}^\sigma &= -\frac{g_{ch}^2}{4\pi} \frac{\Lambda_\sigma^2}{\Lambda_\sigma^2 - m_\sigma^2} m_\sigma \left[Y(m_\sigma r_{ij}) - \frac{\Lambda_\sigma}{m_\sigma} Y(\Lambda_\sigma r_{ij}) \right], \\ v_{ij}^\chi &= \left[Y(m_\chi r_{ij}) - \frac{\Lambda_\chi^3}{m_\chi^3} Y(\Lambda_\chi r_{ij}) \right] \boldsymbol{\sigma}_i \cdot \boldsymbol{\sigma}_j, \quad \chi = \pi, K, \eta, \\ Y(x) &= e^{-x}/x. \end{aligned} \quad (6)$$

$\boldsymbol{\lambda}$ are $SU(3)$ flavor Gell-Mann matrices, m_χ are the masses of Goldstone bosons, Λ_χ are the cut-offs, $g_{ch}^2/4\pi$ is the Goldstone-quark coupling constant.

All the parameters are determined by fitting the meson spectrum, from light to heavy, taking into account only a quark-antiquark component. They are shown in Table I. The calculated masses of the mesons involved in the present work are shown in Table II. Because the spin-orbit interaction is not considered here, we obtained a degenerate eigen-energy for the three P -wave states, 3P_J , $J = 0, 1, 2$.

TABLE II: Meson spectrum (unit: MeV).

		1S_0	3S_1	1P_1	3P_J
$c\bar{c}$	QM	2986.3	3096.4	3416.3	3417.2
	PDG	2979.6	3096.9	3526.2	3510.6
$c\bar{s}$	QM	1953.3	2080.6	2479.3	2482.9
	PDG	1981.0	2112.0	2460.0	2536.0
$s\bar{s}$	QM	824.0	1015.8	1469.1	1481.3
	PDG	957.8	1019.4	1386.0	1426.3

B. The wave function of $c\bar{s}s\bar{c}$ system

There are two physically important structures, meson-meson and diquark-antidiquark, are considered in the present calculation. The wave functions of every structure all consists of four parts: orbital, spin, flavor and color. The wave function of each part is constructed in two steps, first write down the two-body wave functions, then coupling two sub-clusters wave functions to form the four-body one. Because there is no identical particles in the system, the total wave function of the system is the direct product of orbital ($|R_i\rangle$), spin ($|S_j\rangle$), color ($|C_k\rangle$) and flavor ($|F_n\rangle$) wave functions with necessary coupling,

$$|ijkn\rangle = [|R_i\rangle \otimes |S_j\rangle] \otimes |C_k\rangle \otimes |F_n\rangle \quad (7)$$

1. orbital wave function

The orbital wave function of the four-quark system consists of two sub-cluster orbital wave function and the relative motion wave function between two subclusters (1,3 denote quarks and 2,4 denote antiquarks),

$$\begin{aligned} |R_1\rangle &= [[\Psi_{l_1=1}(\mathbf{r}_{12})\Psi_{l_2=0}(\mathbf{r}_{34})]_{l_{12}}\Psi_{L_r}(\mathbf{r}_{1234})]_L^{M_L}, \\ |R_2\rangle &= [[\Psi_{l_1=0}(\mathbf{r}_{12})\Psi_{l_2=1}(\mathbf{r}_{34})]_{l_{12}}\Psi_{L_r}(\mathbf{r}_{1234})]_L^{M_L}, \\ |R_3\rangle &= [[\Psi_{l_1=1}(\mathbf{r}_{13})\Psi_{l_2=0}(\mathbf{r}_{24})]_{l_{12}}\Psi_{L_r}(\mathbf{r}_{1324})]_L^{M_L}, \\ |R_4\rangle &= [[\Psi_{l_1=0}(\mathbf{r}_{13})\Psi_{l_2=1}(\mathbf{r}_{24})]_{l_{12}}\Psi_{L_r}(\mathbf{r}_{1324})]_L^{M_L}, \end{aligned} \quad (8)$$

where the bracket "[]" indicates orbital angular momentum coupling, and L is the total orbital angular momentum which comes from the coupling of L_r , orbital angular momentum of relative motion, and l_{12} , which coupled by l_1 and l_2 , sub-cluster orbital angular momenta. $|R_1\rangle, |R_2\rangle$ donate the orbital wave functions of meson-meson structure, and $|R_3\rangle, |R_4\rangle$ donate the wave functions of diquark-antidiquark structure. In GEM, the radial part of the orbital wave function is expanded by a set of Gaussians:

$$\Psi(\mathbf{r}) = \sum_{n=1}^{n_{\max}} c_n \psi_{nlm}^G(\mathbf{r}), \quad (9a)$$

$$\psi_{nlm}^G(\mathbf{r}) = N_{nl} r^l e^{-\nu_n r^2} Y_{lm}(\hat{\mathbf{r}}), \quad (9b)$$

where N_{nl} are normalization constants,

$$N_{nl} = \left[\frac{2^{l+2} (2\nu_n)^{l+\frac{3}{2}}}{\sqrt{\pi} (2l+1)} \right]^{\frac{1}{2}}. \quad (10)$$

c_n are the variational parameters, which are determined dynamically. The Gaussian size parameters are chosen according to the following geometric progression

$$\nu_n = \frac{1}{r_n^2}, \quad r_n = r_1 a^{n-1}, \quad a = \left(\frac{r_{n_{\max}}}{r_1} \right)^{\frac{1}{n_{\max}-1}}. \quad (11)$$

This procedure enables optimization of the using of Gaussians, as small as possible Gaussians are used.

2. spin wave function

Because of no difference between spin of quark and antiquark, the meson-meson structure has the same spin wave function as the diquark-antidiquark structure. The spin wave functions of the sub-cluster are shown below.

$$\begin{aligned} \chi_{11}^\sigma &= \alpha\alpha, \quad \chi_{10}^\sigma = \frac{1}{\sqrt{2}}(\alpha\beta + \beta\alpha), \quad \chi_{1-1}^\sigma = \beta\beta, \\ \chi_{00}^\sigma &= \frac{1}{\sqrt{2}}(\alpha\beta - \beta\alpha), \end{aligned}$$

Coupling the spin wave functions of two sub-clusters by Clebsch-Gordan coefficients, total spin wave function can be written below,

$$\begin{aligned} |S_1\rangle &= \chi_0^{\sigma 1} = \chi_{00}^\sigma \chi_{00}^\sigma, \\ |S_2\rangle &= \chi_0^{\sigma 2} = \sqrt{\frac{1}{3}}(\chi_{11}^\sigma \chi_{1-1}^\sigma - \chi_{10}^\sigma \chi_{10}^\sigma + \chi_{1-1}^\sigma \chi_{11}^\sigma), \\ |S_3\rangle &= \chi_1^{\sigma 1} = \chi_{00}^\sigma \chi_{11}^\sigma, \\ |S_4\rangle &= \chi_1^{\sigma 2} = \chi_{11}^\sigma \chi_{00}^\sigma, \\ |S_5\rangle &= \chi_1^{\sigma 3} = \frac{1}{\sqrt{2}}(\chi_{11}^\sigma \chi_{10}^\sigma - \chi_{10}^\sigma \chi_{11}^\sigma), \\ |S_6\rangle &= \chi_2^{\sigma 1} = \chi_{11}^\sigma \chi_{11}^\sigma. \end{aligned}$$

the total spin wave function is denoted by $\chi_S^{\sigma i}$, i is the index of the functions, the S is the total spin of the system.

3. flavor wave function

We have two flavor wave functions of the system,

$$\begin{aligned} |F_1\rangle &= (c\bar{s})(s\bar{c}), \\ |F_2\rangle &= (s\bar{s})(c\bar{c}), \\ |F_3\rangle &= (cs)(\bar{c}\bar{s}). \end{aligned}$$

$|F_1\rangle, |F_2\rangle$ is for meson-meson structure, and $|F_3\rangle$ is for diquark-antidiquark structure.

4. color wave function

The colorless tetraquark system has four color wave functions, two for meson-meson structure, $1 \otimes 1$ (C_1), $8 \otimes 8$ (C_2), and two for diquark-antidiquark structure, $\bar{3} \otimes 3$ (C_3) and $6 \otimes \bar{6}$ (C_4).

$$\begin{aligned}
|C_1\rangle &= \sqrt{\frac{1}{9}}(\bar{r}r\bar{r}r + \bar{r}r\bar{g}g + \bar{r}r\bar{b}b + \bar{g}g\bar{r}r + \bar{g}g\bar{g}g \\
&\quad + \bar{g}g\bar{b}b + \bar{b}b\bar{r}r + \bar{b}b\bar{g}g + \bar{b}b\bar{b}b), \\
|C_2\rangle &= \sqrt{\frac{1}{72}}(3\bar{b}r\bar{r}b + 3\bar{g}r\bar{r}g + 3\bar{b}g\bar{g}b + 3\bar{g}b\bar{b}g + 3\bar{r}g\bar{g}r \\
&\quad + 3\bar{r}b\bar{b}r + 2\bar{r}r\bar{r}r + 2\bar{g}g\bar{g}g + 2\bar{b}b\bar{b}b - \bar{r}r\bar{g}g \\
&\quad - \bar{g}g\bar{r}r - \bar{b}b\bar{g}g - \bar{b}b\bar{r}r - \bar{g}g\bar{b}b - \bar{r}r\bar{b}b). \quad (12) \\
|C_3\rangle &= \sqrt{\frac{1}{12}}(rg\bar{r}\bar{g} - rg\bar{g}\bar{r} + gr\bar{g}\bar{r} - gr\bar{r}\bar{g} + rb\bar{r}\bar{b} \\
&\quad - rb\bar{b}\bar{r} + br\bar{b}\bar{r} - br\bar{r}\bar{b} + gb\bar{g}\bar{b} - gb\bar{b}\bar{g} \\
&\quad + bg\bar{b}\bar{g} - bg\bar{g}\bar{b}). \\
|C_4\rangle &= \sqrt{\frac{1}{24}}(2rr\bar{r}\bar{r} + 2gg\bar{g}\bar{g} + 2bb\bar{b}\bar{b} + rg\bar{r}\bar{g} + rg\bar{g}\bar{r} \\
&\quad + gr\bar{g}\bar{r} + gr\bar{r}\bar{g} + rb\bar{r}\bar{b} + rb\bar{b}\bar{r} + br\bar{b}\bar{r} \\
&\quad + br\bar{r}\bar{b} + gb\bar{g}\bar{b} + gb\bar{b}\bar{g} + bg\bar{b}\bar{g} + bg\bar{g}\bar{b}). \quad (13)
\end{aligned}$$

5. total wave function

The total wave functions are obtained by the direct product of wave functions of orbital, spin, color and flavor wave functions. Because we are interested in the states with quantum number $J^P = 1^-$, there must be orbital angular momentum excitation. The experiment suggests that the excited angular quantum number should exist in the one sub-cluster. So we follow the suggestion, set $l_1 = 1, l_2 = 0$ or $l_1 = 0, l_2 = 1$. All the possible channels with the physical contents are listed in the table III. The subscript ‘‘8’’ denotes color octet subcluster, the superscript of diquark/antidiquark is the spin of the sub-cluster, and the subscript is the color representation of subcluster, 3, $\bar{3}$, 6 and $\bar{6}$ denote color triplet, anti-triplet, sextet and anti-sextet.

III. RESULTS

In this section, we present the numerical results of our calculation. As a preliminary calculation, the spin-orbit interaction is not considered in the present calculation. So the states can be classified according to the total spin S of the four-quark system. All the spin of four-quark system $S = 0, 1, 2$ can couple with $L = 1$ to give total angular momentum $J = 1$. Single channel and multi-channel coupling calculations show that no bound state can be formed. Because of the color structures of color-octet channel in meson-meson structure and the diquark-

TABLE III: Index of physical channels for $c\bar{s}s\bar{c}$ system.

$ ijkn\rangle$	$S = 0$	$ ijkn\rangle$	$S = 1$
1111)	$D_s\bar{D}_{s1}(2460)$	1311)	$D_s\bar{D}_{sj}$
1121)	$[D_s]_8[\bar{D}_{s1}(2460)]_8$	1321)	$[D_s]_8[\bar{D}_{sj}]_8$
1211)	$D_s^*\bar{D}_{sj}$	1411)	$D_s^*\bar{D}_{s1}(2460)$
1221)	$[D_s^*]_8[\bar{D}_{sj}]_8$	1421)	$[D_s^*]_8[\bar{D}_{s1}(2460)]_8$
2111)	$D_{s1}(2460)\bar{D}_s$	1511)	$D_s^*\bar{D}_{sj}$
2121)	$[D_{s1}(2460)]_8[\bar{D}_s]_8$	1521)	$[D_s^*]_8[\bar{D}_{sj}]_8$
2211)	$D_{sj}\bar{D}_s^*$	2311)	$D_{s1}(2460)\bar{D}_s^*$
2221)	$[D_{sj}]_8[\bar{D}_s^*]_8$	2321)	$[D_{s1}(2460)]_8[\bar{D}_s^*]_8$
1112)	$\eta' h_c$	2411)	$D_{sj}\bar{D}_s$
1122)	$[\eta']_8[h_c]_8$	2421)	$[D_{sj}]_8[\bar{D}_s]_8$
1212)	$\phi'\chi_{cj}$	2511)	$D_{sj}\bar{D}_s^*$
1222)	$[\phi']_8[\chi_{cj}]_8$	2521)	$[D_{sj}]_8[\bar{D}_s^*]_8$
2112)	$h\eta_c$	1312)	$\eta'\chi_{cj}$
2122)	$[h]_8[\eta_c]_8$	1322)	$[\eta']_8[\chi_{cj}]_8$
2212)	$f_j J/\psi$	1412)	ϕh_c
2222)	$[f_j]_8[J/\psi]_8$	1422)	$[\phi]_8[h_c]_8$
3133)	$[sc]_3^0[\bar{s}\bar{c}]_3^0$	1512)	$\phi\chi_{cj}$
3143)	$[sc]_6^0[\bar{s}\bar{c}]_6^0$	1522)	$[\phi]_8[\chi_{cj}]_8$
3233)	$[sc]_3^1[\bar{s}\bar{c}]_3^1$	2312)	hJ/ψ
3243)	$[sc]_6^1[\bar{s}\bar{c}]_6^1$	2322)	$[h]_8[J/\psi]_8$
4133)	$[sc]_3^0[\bar{s}\bar{c}]_3^0$	2412)	$f_j\eta_c$
4143)	$[sc]_6^0[\bar{s}\bar{c}]_6^0$	2422)	$[f_j]_8[\eta_c]_8$
4233)	$[sc]_3^1[\bar{s}\bar{c}]_3^1$	2512)	$f_j J/\psi$
4243)	$[sc]_6^1[\bar{s}\bar{c}]_6^1$	2522)	$[f_j]_8[J/\psi]_8$
ijkn)	$S = 2$	3333)	$[sc]_3^0[\bar{s}\bar{c}]_3^0$
1611)	$D_s^*\bar{D}_{sj}$	3343)	$[sc]_6^0[\bar{s}\bar{c}]_6^0$
1621)	$[D_s^*]_8[\bar{D}_{sj}]_8$	3433)	$[sc]_3^1[\bar{s}\bar{c}]_3^1$
2611)	$D_{sj}\bar{D}_s^*$	3443)	$[sc]_6^1[\bar{s}\bar{c}]_6^0$
2621)	$[D_{sj}]_8[\bar{D}_s^*]_8$	3533)	$[sc]_3^1[\bar{s}\bar{c}]_3^1$
1612)	$\phi\chi_{cj}$	3543)	$[sc]_6^1[\bar{s}\bar{c}]_6^0$
1622)	$[\phi]_8[\chi_{cj}]_8$	4333)	$[sc]_3^0[\bar{s}\bar{c}]_3^1$
2612)	$f_j J/\psi$	4343)	$[sc]_6^0[\bar{s}\bar{c}]_6^0$
2622)	$[f_j]_8[J/\psi]_8$	4433)	$[sc]_3^1[\bar{s}\bar{c}]_3^0$
3633)	$[sc]_3^1[\bar{s}\bar{c}]_3^1$	4443)	$[sc]_6^0[\bar{s}\bar{c}]_6^0$
3643)	$[sc]_6^1[\bar{s}\bar{c}]_6^0$	4533)	$[sc]_3^1[\bar{s}\bar{c}]_3^1$
4633)	$[sc]_3^1[\bar{s}\bar{c}]_3^1$	4543)	$[sc]_6^1[\bar{s}\bar{c}]_6^0$
4643)	$[sc]_6^1[\bar{s}\bar{c}]_6^0$		

antiquark structure, the system cannot fall apart directly. So in the single channel calculation, we always obtain stable energies for these channels. To see if these states are genuine resonances or not, the real-scaling method [23, 24] is employed. In this method, the Gaussian size parameters r_n for the basis functions between two sub-clusters for the color-singlet channels are scaled by multiplying a factor α , i.e. $r_n \rightarrow \alpha r_n$. Then, any continuum state will fall off towards its threshold, while a compact resonant state should not be affected by the variation of α .

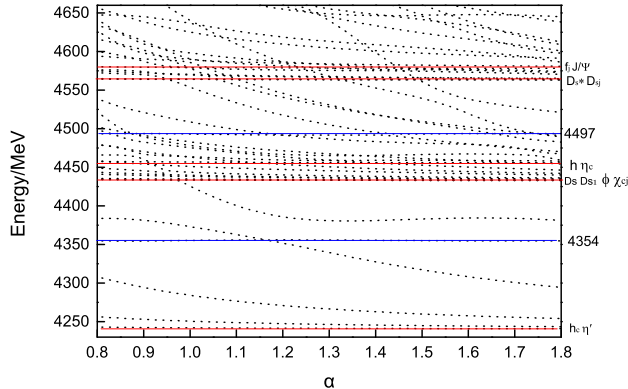


FIG. 1: Energy spectrum of 1P_1 states.

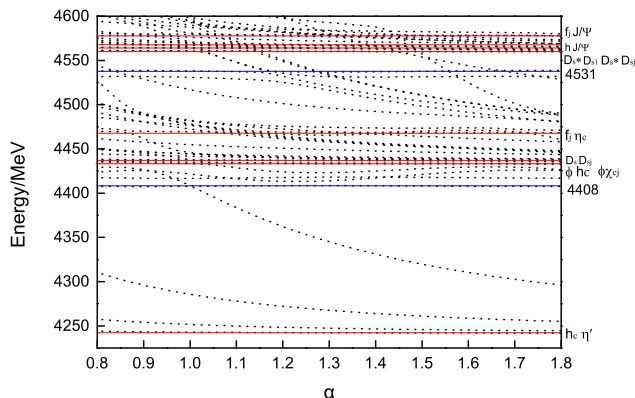


FIG. 2: Energy spectrum of 3P_1 states.

The results for $S = 0, 1, 2$ are shown in Figs. 1, 2 and 3. In each figure, all the thresholds are marked with a line and physical contents. the possible resonance are also highlighted with a line and its energy, and only the lowest one or two resonance states are displayed. From the figures, we can see that the thresholds are all shown

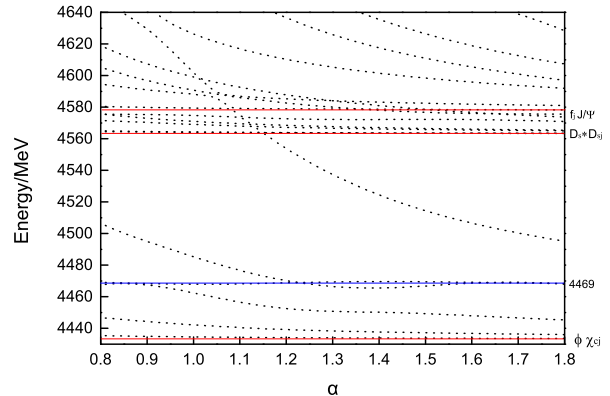


FIG. 3: Energy spectrum of 3P_1 states.

up with horizontal lines. Besides, there are genuine resonances, their energies are stable with the increasing α . For $S = 0$, we obtain two resonances with energies, 4354 and 4497 MeV below 4650 MeV. For $S = 1$, two resonances with energies, 4408 and 4531 MeV are shown. There is only one resonance with energy 4469 MeV below 4650 MeV.

In the quark model calculation, the masses and decay properties of hadrons can be described well. However the description cannot be perfect. there are always some deviations. We take these deviations as our systematic errors of our calculations. From table II, we can see that the systematic errors in the present calculation are 60~100 MeV. Taking into account of the systematic error, we find that the resonance with energy 4531 can be a candidate of the newly reported state $Y(4626)$.

TABLE IV: The average separations between any quark/antiquark pairs (unit: fm).

state	$r_{c\bar{s}}$	r_{cs}	$r_{c\bar{c}}$	$r_{s\bar{s}}$	$r_{s\bar{c}}$	$r_{s\bar{c}}$
$R(4354)$	0.9	0.9	0.4	0.9	0.9	0.9
$R(4497)$	0.7	0.8	0.6	0.9	0.8	0.7
$R(4408)$	0.7	1.4	1.4	1.4	1.4	0.7
$R(4531)$	0.7	0.8	0.7	1.0	0.8	0.7
$R(4469)$	0.9	0.9	0.4	0.9	0.9	0.9

To explore the structures of the resonances, the average separations between any quark/antiquark pair are calculated, the results are shown in table IV. From the table, we find that all the separation are not larger than 1.0 fm except for the state $R(4408)$, so these states are compact objects. For the state $R(4408)$, we have small separations $r_{c\bar{s}}$ and $r_{s\bar{c}}$, and a little large separations r_{cs} , $r_{c\bar{c}}$, $r_{s\bar{s}}$ and $r_{s\bar{c}}$, so it is a molecule. For the state $R(4531)$,

a candidate of the state $Y(4626)$, all the separation are around 0.8 fm, so it is a compact tetraquark state. The wavefunction of the state supports the picture, where the configurations with colorful subclusters dominant.

IV. SUMMARY

In the framework of the chiral constituent quark model, we study systematically $J^P = 1^- \bar{c}\bar{s}s\bar{c}$ states. Two different structures, meson-meson structure and diquark-antidiquark, with all possible color, flavor, spin configurations are taken into account. In the absence of spin-orbit interaction, we found that there is no bound state for this system. However, the resonances are possible. To distinguish the genuine resonances from the discretized scattering states, the real-scaling method is employed. The calculations show that there are five resonance states with $J^P = 1^-$ and $S = 0, 1, 2$. One state with molecular

structure, and other states are all have a compact structure. The newly observed state $Y(4620)$ can be described as a $c\bar{s}c\bar{c}$ compact tetraquark state.

When the spin-orbit and tensor interactions are included, all the states with $S = 0$, $S = 1$ and $S = 2$ will be mixed up. Clearly, further calculation is expected. Whether the state can survive after invoking spin-orbit and tensor interactions? If these states survive, the decay widths have to be calculated to check the compatibility with the experimental data. Are there other explanations of the state $Y(4620)$? These are our future work.

Acknowledgments

This work is supported partly by the National Natural Science Foundation of China under Contract Nos. 11675080, 11175088 and 11535005.

-
- [1] S. K. Choi *et al.* [Belle Collaboration], Phys. Rev. Lett. **91**, 262001 (2003).
 - [2] K. Abe *et al.* [Belle Collaboration], Phys. Rev. Lett. **94**, 182002 (2005).
 - [3] B. Aubert *et al.* [BaBar Collaboration], Phys. Rev. Lett. **95**, 142001 (2005).
 - [4] S. K. Choi *et al.* [Belle Collaboration], Phys. Rev. Lett. **100**, 142001 (2008).
 - [5] C. Z. Yuan *et al.* [Belle Collaboration], Phys. Rev. Lett. **99**, 182004 (2007).
 - [6] R. Mizuk *et al.* [Belle Collaboration], Phys. Rev. D **78**, 072004 (2008).
 - [7] T. Aaltonen *et al.* [CDF Collaboration], Phys. Rev. Lett. **102**, 242002 (2009).
 - [8] R. Aaij *et al.* [LHCb Collaboration], JHEP **1907**, 035 (2019).
 - [9] S. Jia *et al.* [Belle Collaboration], arXiv:1911.00671 [hep-ex].
 - [10] H. X. Chen, E. L. Cui, W. Chen, X. Liu and S. L. Zhu, Eur. Phys. J. C **77**, no. 3, 160 (2017).
 - [11] C. Deng, J. Ping, H. Huang and F. Wang, Phys. Rev. D **98**, no. 1, 014026 (2018).
 - [12] Y. Yang and J. Ping, Phys. Rev. D **99**, no. 9, 094032 (2019).
 - [13] Q. F. Lü and Y. B. Dong, Phys. Rev. D **94**, no. 7, 074007 (2016).
 - [14] J. Wu, Y. R. Liu, K. Chen, X. Liu and S. L. Zhu, Phys. Rev. D **94**, no. 9, 094031 (2016).
 - [15] F. Stancu, J. Phys. G **37**, 075017 (2010).
 - [16] P. G. Ortega, J. Segovia, D. R. Entem and F. Fernandez, Phys. Rev. D **94**, no. 11, 114018 (2016).
 - [17] J. Vijande, F. Fernandez and A. Valcarce, J. Phys. G **31**, 481 (2005).
 - [18] Y. Yang, C. Deng, H. Huang and J. Ping, Mod. Phys. Lett. A **23**, 1819 (2008).
 - [19] Y. Yang, C. Deng, J. Ping and T. Goldman, Phys. Rev. D **80**, 114023 (2009).
 - [20] X. Chen and J. Ping, Eur. Phys. J. C **76**, no. 6, 351 (2016).
 - [21] X. Chen, J. Ping, C. D. Roberts and J. Segovia, Phys. Rev. D **97**, no. 9, 094016 (2018).
 - [22] Y. Tan and J. Ping, Phys. Rev. D **100**, no. 3, 034022 (2019).
 - [23] J. Simons, The Journal of Chemical Physics **75** (1981) 2465C2467.
 - [24] Q. Meng, E. Hiyama, K. U. Can, P. Gubler, M. Oka, A. Hosaka and H. Zong, Phys. Lett. B **798**, 135028 (2019).